Acta Crystallographica Section A
Foundations and Advances
ISSN 2053-2733

Received 14 May 2014
Accepted 25 July 2014

Icosahedral symmetry breaking: C_{60} to C_{78}, C_{96} and to related nanotubes

Mark Bodner,[a] Emmanuel Bourret,[b] Jiri Patera[a,b] and Marzena Szajewska[a,b,c]*

[a]MIND Research Institute, 111 Academy Drive, Irvine, California 92617, USA, [b]Centre de recherches mathématiques, Université de Montréal, CP 6128, Centre-ville, Montréal, H3C 3J7, Québec, Canada, and [c]Institute of Mathematics, University of Bialystok, Akademicka 2, PL-15-267, Bialystok, Poland. Correspondence e-mail: m.szajewska@math.uwb.edu.pl

Exact icosahedral symmetry of C_{60} is viewed as the union of 12 orbits of the symmetric subgroup of order 6 of the icosahedral group of order 120. Here, this subgroup is denoted by A_2 because it is isomorphic to the Weyl group of the simple Lie algebra A_2. Eight of the A_2 orbits are hexagons and four are triangles. Only two of the hexagons appear as part of the C_{60} surface shell. The orbits form a stack of parallel layers centered on the axis of C_{60} passing through the centers of two opposite hexagons on the surface of C_{60}. By inserting into the middle of the stack two A_2 orbits of six points each and two A_2 orbits of three points each, one can match the structure of C_{78}. Repeating the insertion, one gets C_{96}; multiple such insertions generate nanotubes of any desired length. Five different polytopes with 78 carbon-like vertices are described; only two of them can be augmented to nanotubes.

1. Introduction

The present paper is an independent continuation of the work reported by Bodner *et al.* (2013), where the icosahedral symmetry of the fullerene C_{60} was broken to the subgroup H_2 of the icosahedral group H_3, providing a mechanism for the generation of larger fullerenes of the form C_{60+N10}. The subject of our study here is icosahedral symmetry breaking to the subgroup A_2, more precisely to the Weyl group of the simple Lie algebra A_2, which is the finite symmetry group of order 6 isomorphic to the symmetric group of three elements.

While Bodner *et al.* (2013) reported the fullerene polytopes related to C_{60} were C_{70}, C_{80}, C_{90} and related nanotubes, in this paper the fullerenes arising from C_{60} are C_{78}, C_{96}, C_{114} and other related types of nanotubes. In general, the situation here is more complicated than reported by Bodner *et al.* (2013), as there are five different fullerene C_{78} polytopes. Two of them are the result of two variants of the symmetry breaking $H_3 \rightarrow A_2$, each of them leading to a series of larger fullerenes and nanotubes (Dresselhaus *et al.*, 1996; Harris, 1999; Fowler & Manolopoulos, 2007; Cataldo *et al.*, 2011). The remaining three C_{78} polytopes have no detectable subgroup symmetry and no related nanotubes.

The five types of C_{78} polytopes, C_{78}(I), C_{78}(II), ..., C_{78}(V)[1], are distinguished by the pairs of the nearest pentagons on their surface 'central belt', *i.e.* the three rings of hexagons and pentagons in the middle of the polytope oriented along the α_3 direction. While C_{78}(I) and C_{78}(II) can be extended to larger polytopes and to nanotubes of any desired length by insertion of a corresponding number of additional rings of nine hexagons into the middle of the structure, the polytopes C_{78}(III), C_{78}(IV) and C_{78}(V) cannot be extended further in any systematic way.

In this paper, we continue to pursue the general idea of symmetry breaking, or symmetry reduction, as is often done in science (Ramond, 2011) as a mechanism for the generation of specific large fullerenes existing in nature (Balasubramanian, 1991; Wang *et al.*, 2007; Fowler & Manolopoulos, 2007; Lin *et al.*, 1999, 2006; Zhang *et al.*, 1993). Large symmetry, say G, is broken or reduced to the symmetry of one of the subgroups, say $G' \subset G$. Here the symmetry group G is the icosahedral group (denoted H_3) of order 120, acting in the three-dimensional real Euclidean space $\mathbb{R}^3$.

Here we explore one of the three 'natural' avenues of breaking H_3 symmetry. The group H_3 is generated by three reflection operations called here r_1, r_2 and r_3 (for an elaboration on these reflections see §2.2). There are three ways of breaking H_3 to retain only two of the three reflections as generating elements for the subgroup $G' \subset H_3$. Specifically we have the following possibilities for G':

$$r_2, r_3 \text{ generate } G' = H_2 |H_2| = 10, \tag{1}$$

$$r_1, r_2 \text{ generate } G' = A_2 |A_2| = 6, \tag{2}$$

$$r_1, r_3 \text{ generate } G' = A_1 \times A_1 \quad |A_1 \times A_1| = 4, \tag{3}$$

where we have introduced notation for the three types of the subgroups G' and show the order $|G'|$ of G'. The three ways of

[1] For clarity, we specify here the point groups of the C_{78} isomers. In the Schönflies convention, C_{78}(I) and C_{78}(II) are D_{3h}, C_{78}(III) is D_3, and C_{78}(IV) and C_{78}(V) are C_{2v}. These are given in paper by Fowler & Manolopoulos (2007).

symmetry breaking we mentioned above do not exhaust all possible symmetry breakings of H_3; however, they appear more naturally or less arbitrary having no built-in parameters to fix.

The case (1) was studied by Bodner *et al.* (2013, 2014), which led from C_{60} to the generation of the fullerenes C_{70}, C_{80}, C_{90}, ... and to corresponding nanotubes.

The case (2) is the subject of the present paper.

The case (3) was not studied as a symmetry-breaking problem. It will be considered elsewhere.

If the icosahedral symmetry breaking is guided by the subgroup A_2, the polytope with broken symmetry closest to C_{60} is the fullerene C_{78}. It turns out that there are two possible versions of the symmetry-breaking mechanism, leading to two different C_{78} polytopes. Both versions can be extended by breaking the symmetry an arbitrary number of times, leading to the generation of nanotubes of any desired length. However, five different C_{78} molecules have been identified theoretically, with the two considered here being among them. All are near spherical shells with surfaces built by hexagons and pentagons [see, for example, Table A in the book by Fowler & Manolopoulos (2007)]. In the cases of the three additional C_{78} polytopes, one finds no large subgroup of the icosahedral group, whose symmetry would be retained during the symmetry breaking.

In addition to the fullerene C_{60}, defined by its dominant point $\omega_1 + \omega_2$, there are two other polytopes with exact icosahedral symmetry and 60 vertices. We do not call those polytopes fullerenes. Their dominant points are $\omega_2 + \omega_3$ and $\omega_1 + \omega_3$. The two cases are easily distinguished from the fullerene C_{60} by their 2-faces (Champagne *et al.*, 1995). In the one case these faces are decagons and triangles, while in the second case the 2-faces are pentagons, squares and triangles, while the C_{60} fullerene is built from pentagons and hexagons. The general method of identification and description of faces of n-dimensional polytopes was found by Champagne *et al.* (1995). For an extensive application of the method see Szajewska (2014).

It was shown in the paper by Bodner *et al.* (2013) that there exists a continuum of different polytopes that display an exact icosahedral symmetry and have 60 vertices. They are called the 'twisted fullerenes'. Their shell is formed by 12 regular pentagons and 20 nonregular hexagons which have three sides of one length and three sides of another length. It appears that none of these C_{60} stereoisomers allow extension to nanotubes.

2. The fullerene C_{60}

The three reflections in mirrors that have a common point at the origin of the three-dimensional Euclidean space $\mathbb{R}^3$ generate reflection groups in $\mathbb{R}^3$. Relative angles of the mirrors determine whether the group is finite or not and which group it is. The angles between the mirrors are specified by the relative angles of the three normal vectors to the mirrors α_1, α_2 and α_3. Fixing for convenience the length of the three α-vectors to be the same, then the angles are read from the Coxeter diagram (see Fig. 1), one has the α-basis of the icosahedral symmetry in $\mathbb{R}^3$. The α-basis $\{\alpha_1, \alpha_2, \alpha_3\}$ of vector normals to the reflection mirrors define the icosahedral group.

The α-basis is defined by the matrix C of the scalar products of the basis vectors,

$$C = \big(C_{jk}\big) = (\langle \alpha_j, \alpha_k \rangle) = \begin{pmatrix} 2 & -1 & 0 \\ -1 & 2 & -\tau \\ 0 & -\tau & 2 \end{pmatrix},$$
$$\tau = \tfrac{1}{2}\big[1 + (5)^{1/2}\big] = 2\cos \pi/5. \qquad (4)$$

2.1. Icosahedral bases in $\mathbb{R}^3$

A considerable simplification of the description of the polytopes with icosahedral symmetry can be achieved when bases defined by the symmetry group are used, since the bases are not orthogonal.

Besides the α-basis, we use the ω-basis that is reciprocal, or equivalently, dual to the α-basis. It is defined by the requirement

$$\langle \alpha_j, \omega_k \rangle = \delta_{jk}, \quad j, k = 1, 2, 3. \qquad (5)$$

It is given by the matrix C^{-1}, inverse to C. Matrix elements of C^{-1} are the scalar products of the vectors of the ω-basis (Champagne *et al.*, 1995)

$$(C^{-1}_{jk}) = (\langle \omega_j, \omega_k \rangle) = \frac{1}{2}\begin{pmatrix} 2+\tau & 2+2\tau & 1+2\tau \\ 2+2\tau & 4+4\tau & 2+4\tau \\ 1+2\tau & 2+4\tau & 3+3\tau \end{pmatrix}. \qquad (6)$$

Of practical importance are the relations:

$$\alpha_j = \sum_{k=1}^{3} C_{jk}\omega_k, \quad \omega_k = \sum_{j=1}^{3} C^{-1}_{kj}\alpha_j. \qquad (7)$$

It should be noted that requirement (5) does not imply that α_k and ω_k are collinear for any k = 1, 2 or 3. Indeed, the vectors ω_k are of different length (6). In particular,

$$\omega_1 = \tfrac{1}{2}(2+\tau)\alpha_1 + (1+\tau)\alpha_2 + \tfrac{1}{2}(1+2\tau)\alpha_3,$$
$$\omega_2 = (1+\tau)\alpha_1 + (2+2\tau)\alpha_2 + (1+2\tau)\alpha_3,$$
$$\omega_3 = \tfrac{1}{2}(1+2\tau)\alpha_1 + (1+2\tau)\alpha_2 + \tfrac{3}{2}(1+\tau)\alpha_3. \qquad (8)$$

Of interest to us here is the subgroup A_2 of H_3. It is the dihedral group of order 6, and it is isomorphic to the symmetric group of three elements. It is conveniently fixed inside H_3 by choosing α_1 and α_2 to be its α-basis, *i.e.* vectors normal to the refection mirrors of A_2. As the dual basis we

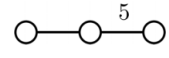

Figure 1
Coxeter diagram of H_3. Its nodes are taken to stand for the basis vectors of the α-basis, numbered from left to right. Connecting lines specify the angles between basis vectors: a single line without the number means that the angle is 120°, a line with the number 5 means 144°, and the absence of a direct connection implies orthogonality of the two basis vectors. It is also sometimes useful to read the nodes of the diagram as the vectors of the ω-basis, or for the reflections r_1, r_2, r_3 in mirrors orthogonal to vectors of the α-basis and intersecting at the origin of $\mathbb{R}^3$.

choose ω_1 and ω_2 because they satisfy requirement (5) for $j, k = 1, 2$. Note that by requirement (5), the direction orthogonal to the plane spanned by ω_1 and ω_2 is the direction of α_3.

2.2. Icosahedral reflections

A reflection is called icosahedral provided it is a reflection in one of the three mirrors whose orientation is fixed by the vector normals α_1, α_2, α_3. We denote by r_1, r_2 and r_3 the corresponding reflection operations. Any point $x \in \mathbb{R}^3$ is reflected according to

$$r_k x = x - \langle x, \alpha_k \rangle \alpha_k, \qquad k = 1, 2, 3, \qquad x \in \mathbb{R}^3. \quad (9)$$

In particular, $r_k \alpha_j = \alpha_j - \langle \alpha_k, \alpha_j \rangle \alpha_k$ and also $r_k \omega_j = \omega_j - \delta_{jk} \alpha_k$. By explicit calculation one can check the following identities:

$$r_1^2 = r_2^2 = r_3^2 = 1, \quad (r_1 r_2)^3 = 1, \quad (r_1 r_3)^2 = 1, \quad (r_2 r_3)^5 = 1, \quad (10)$$

where 1 stands for an identity operation.

Repeated application of the reflection operations (9) to any point x generate precisely one orbit of the H_3 group. Any point x cannot belong to two orbits of H_3. The number of distinct points in any orbit is easily found, provided x is given relative to the ω-basis (Champagne *et al.*, 1995). As usual, we interpret the points of the orbit as vertices of an icosahedral polytope in $\mathbb{R}^3$. The orbit of 60 elements/vertices arises when $x = a\omega_1 + b\omega_2$ with $a, b > 0$. If in addition, we have $a = b$, the polytope is the fullerene C_{60}. If $a \neq b$, one gets the 'twisted' polytope of the paper by Bodner *et al.* (2014), still displaying exact icosahedral symmetry, but whose edges between hexagons are of different length than the edges separating hexagons and pentagons.

The faces of C_{60} have been described previously (Champagne *et al.*, 1995; Bodner *et al.*, 2013, 2014) together with a method for finding them. There are 60 faces of dimension 0 (vertices), 20 hexagonal faces and 12 pentagonal ones (faces of dimension 2), and 30 edges between two hexagons and 60 edges separating hexagons and pentagons (faces of dimension 1).

3. The A_2 orbits of vertices of C_{60}

The vertices of C_{60} are generated by the reflections (9) from any of its points, although it is practical to identify an orbit by its unique dominant point, the only orbit point that has non-negative coordinates in the ω-basis. Therefore the 60 points belong to a single orbit of vertices of the icosahedral group H_3. All 60 vertices of the polytope are listed in the ω-basis of H_3 by Bodner *et al.* (2013, 2014). However, when one looks at the same set of 60 vertices from the perspective of a subgroup of H_3, in the present case the subgroup A_2, the vertices decompose into several orbits of A_2.

Here the list of 60 vertices of C_{60} is reproduced from Bodner *et al.* (2013, 2014).

$\boxed{\pm(1, 1, 0)}$	$\pm(-1, 2, 0)$	$\pm(2, -1, \tau)$
$\pm(1, -2, 2\tau)$	$\pm(\tau, -2-\tau, 1+2\tau)$	$\boxed{\pm(-1, -1, 2\tau)}$
$\pm(-2, 2+\tau, -\tau)$	$\pm(2+\tau, -\tau, 1)$	$\boxed{\pm(1, 2\tau, -2\tau)}$
$\pm(-1, 1+2\tau, -2\tau)$	$\pm(-2, 1, \tau)$	$\pm(-2-\tau, 2, 1)$
$\boxed{\pm(2+\tau, 0, -1)}$	$\pm(1+2\tau, -2\tau, 2)$	$\pm(2\tau, -1-2\tau, 2+\tau)$
$\boxed{\pm(1+2\tau, 0, -2)}$	$\boxed{\pm(\tau, 2\tau, -1-2\tau)}$	$\pm(-2-\tau, 2+\tau, -1)$
$\pm(-1-2\tau, 1, 2)$	$\boxed{\pm(-\tau, -2, 1+2\tau)}$	$\boxed{\pm(0, -2-\tau, 3\tau)}$
$\boxed{\pm(2\tau, \tau, -2-\tau)}$	$\pm(-\tau, 3\tau, -1-2\tau)$	$\pm(3\tau, -2\tau, 1)$
$\boxed{\pm(-2\tau, -1, 2+\tau)}$	$\boxed{\pm(2, -\tau, -\tau)}$	$\pm(3\tau, -\tau, -1)$
$\pm(-2\tau, 3\tau, -2-\tau)$	$\boxed{\pm(0, 1+2\tau, -3\tau)}$	$\pm(-1-2\tau, 1+2\tau, -2)$

The points that are in boxes specify the orbits of the subgroup A_2 of H_3. They are distinguished by the signs of their first and second coordinates. These signs coincide. Therefore, the points taken with the non-negative signs of the first two coordinates are the highest ('dominant') points on the orbit. When both coordinates are positive, its A_2 orbit has six points. When one of the coordinates is zero, its orbit consists of three points. There are eight orbits of six points and four orbits of three points.

During the transformation of a vector given relative to the basis $\{\omega_1, \omega_2, \omega_3\}$ to the basis $\{\omega_1, \omega_2, \alpha_3\}$, dominant vectors remain dominant in their orbits, because the transformation leaves the first two coordinates unchanged.

Suppose (a, b, c) is given relative to the basis $\{\omega_1, \omega_2, \omega_3\}$. In order to transform it to the basis $\{\omega_1, \omega_2, \alpha_3\}$, one proceeds as follows,

$$\begin{aligned}(a, b, c)&\begin{pmatrix} 1 & 0 & \frac{1}{2}+\tau \\ 0 & 1 & 1+2\tau \\ 0 & 0 & \frac{3}{2}+\frac{3}{2}\tau \end{pmatrix}\begin{pmatrix} a \\ b \\ c \end{pmatrix} \\ &= \big(a, b, a(\tfrac{1}{2}+\tau) + b(1+2\tau) + c(\tfrac{3}{2}+\tfrac{3}{2}\tau)\big) \\ &= \big(a, b, \tfrac{1}{2}(a+2b+3c) + \tau\tfrac{1}{2}(2a+4b+3c)\big).\end{aligned}$$

Thus one gets the following specific transformations:

$$(1, 1, 0) \longrightarrow (1, 1, \tfrac{3}{2}+3\tau), \quad (2, \tau, -\tau) \longrightarrow (2, \tau, \tfrac{3}{2}+2\tau), \ldots$$

Rewriting the vertices of C_{60} in the A_2 basis, *i.e.* $\{\omega_1, \omega_2, \alpha_3\}$, we have:

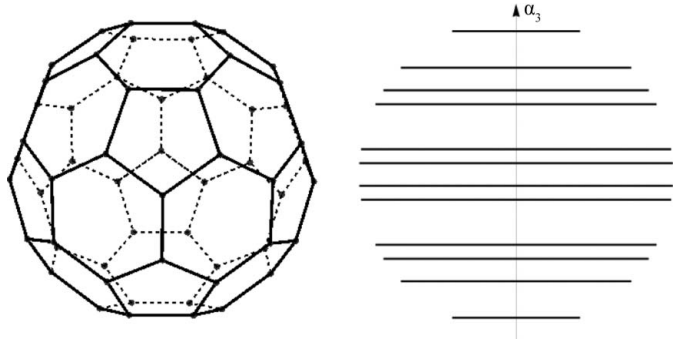

Figure 2
The polytope C_{60} viewed from the direction parallel to the plane spanned by ω_1 and ω_2. The orbits of A_2 appear as horizontal segments ('stack of pancakes').

$$\boxed{\pm(1, 1, \tfrac{3}{2}+3\tau)} \quad \pm(-\tau, 3\tau, \tfrac{1}{2}) \quad \boxed{\pm(-1, -1, \tfrac{3}{2}+3\tau)}$$
$$\pm(2, -1, \tfrac{3}{2}+3\tau) \quad \pm(-2-\tau, 2+\tau, \tfrac{1}{2}+2\tau) \quad \pm(1, -2, \tfrac{3}{2}+3\tau)$$
$$\pm(-3\tau, \tau, \tfrac{1}{2}) \quad \pm(2+\tau, -\tau, \tfrac{3}{2}+2\tau) \quad \pm(\tau, -2-\tau, \tfrac{3}{2}+2\tau)$$
$$\boxed{\pm(0, -1-2\tau, -\tfrac{1}{2}+\tau)} \quad \boxed{\pm(1, 2\tau, \tfrac{3}{2}+\tau)} \quad \pm(3\tau, -2\tau, \tfrac{1}{2})$$
$$\boxed{\pm(2+\tau, 0, \tfrac{1}{2}+2\tau)} \quad \pm(1+2\tau, -2\tau, \tfrac{3}{2}+\tau)$$
$$\pm(2\tau, -1-2\tau, \tfrac{3}{2}+\tau) \quad \pm(-2, 1, \tfrac{3}{2}+3\tau) \quad \boxed{\pm(\tau, 2\tau, \tfrac{1}{2})}$$
$$\boxed{\pm(-\tau, -2, \tfrac{3}{2}+2\tau)} \quad \pm(-1-2\tau, 1, \tfrac{3}{2}+\tau)$$
$$\boxed{\pm(1+2\tau, 0, -\tfrac{1}{2}+\tau)} \quad \pm(-1, 2, \tfrac{3}{2}+3\tau) \quad \boxed{\pm(-2\tau, -\tau, \tfrac{1}{2})}$$
$$\boxed{\pm(-2\tau, -1, \tfrac{3}{2}+\tau)} \quad \pm(-2-\tau, 2, \tfrac{3}{2}+2\tau) \quad \boxed{\pm(0, -2-\tau, \tfrac{1}{2}+2\tau)}$$
$$\boxed{\pm(2, \tau, \tfrac{3}{2}+2\tau)} \quad \pm(2\tau, -3\tau, \tfrac{1}{2}) \quad \pm(-2, 2+\tau, \tfrac{3}{2}+2\tau)$$
$$\pm(-1, 1+2\tau, \tfrac{3}{2}+\tau) \quad \pm(-1-2\tau, 1+2\tau, -\tfrac{1}{2}+\tau) \tag{11}$$

Ordering the A_2 orbits by their α_3 coordinate, we find that the upper half of C_{60} consisting of the orbits (identified by their dominant weights)

$$\boxed{(1, 1, \tfrac{3}{2}+3\tau)}, \quad \boxed{(2, \tau, \tfrac{3}{2}+2\tau)}, \quad \boxed{(2+\tau, 0, \tfrac{1}{2}+2\tau)},$$
$$\boxed{(1, 2\tau, \tfrac{3}{2}+\tau)}, \quad \boxed{(1+\tau, 0, -\tfrac{1}{2}+\tau)}, \quad \boxed{(\tau, 2\tau, \tfrac{1}{2})},$$

while in the lower half the dominant weights of the A_2 orbits of C_{60} have the sign of the third coordinate reversed, and the first two coordinates interchanged.

$$\boxed{(2\tau, \tau, -\tfrac{1}{2})}, \quad \boxed{(0, 1+\tau, \tfrac{1}{2}-\tau)}, \quad \boxed{(2\tau, 1, -\tfrac{3}{2}-\tau)},$$
$$\boxed{(0, 2+\tau, -\tfrac{1}{2}-2\tau)}, \quad \boxed{(\tau, 2, -\tfrac{3}{2}-2\tau)}, \quad \boxed{(1, 1, -\tfrac{3}{2}-3\tau)},$$

3.1. C_{60} as the stack of A_2 pancakes

Looking at C_{60} along the plane spanned by ω_1 and ω_2, the orbits of A_2 are viewed as horizontal segments, while the vertical direction is that of α_3. The structure is particularly visible in Fig. 2.

4. Symmetry breaking $C_{60} \rightarrow A_2$

Breaking the icosahedral symmetry H_3 to that of A_2 (dihedral group of order 6) is the main subject here. It is applied to the reduction of the icosahedral symmetry H_3 of C_{60} to the 12 orbits of A_2. The reduction yields eight hexagonal orbits of A_2 and four triangular ones.

There are five different polytopes with 78 C atoms forming 29 hexagons and 12 pentagons on their surfaces. In order to distinguish the five cases, we use the notation C_{78}(I), C_{78}(II), ..., C_{78}(V), and these are shown in Figs. 3, 4, 5 and 6, respectively.

Breaking of the H_3 symmetry to its subgroup A_2 amounts to two operations: (i) insertion of several additional orbits of A_2 into the middle of the structure as in Fig. 2, and (ii) appropriate displacement of the upper and lower halves of C_{60} along the α_3-axis vector. The two operations are subject to the general requirement that the shell of the resulting polytope is formed as before by regular hexagons and 12 pentagons.

4.1. Polytopes C_{78}(I) and C_{78}(II)

Only the polytopes C_{78}(I) (Fig. 3) and C_{78}(II) (Fig. 4) occur as a result of the symmetry breaking $H_3 \rightarrow A_2$. They correspond to two possible variants of insertions of the middle belt into C_{60} (see Figs. 3 and 4). The two cases can be distinguished by looking at the pairs of nearest pentagons. In C_{78}(I) they are linked by an edge of the polytope, while in C_{78}(II) any two nearest pentagons are connected by a hexagon.

The middle belts of Figs. 3 and 4 display a mismatch between the vertices and edges of pentagons and of hexagons. The mismatch has a contribution from three different factors: (i) unwrapping the belt to a plane from the rounded C_{78}, (ii) the angles between edges within pentagons and/or hexagons can be distorted and (iii) the edges of the polytope may be bent and not of the same length. Only very precise measurement of real carbon polytopes may reveal how much each of these three factors contribute to the mismatch.

The central ring of nine hexagons in Figs. 3 and 4 can be extended to three hexagonal rings, forming C_{114}. Adjacent rings of six hexagons and three pentagons from both sides of the hexagon rings would fit the triple ring. Continuing further, one can build $C_{60+18(2k+1)}$ by inserting $2k+1$ hexagonal rings. At some k such extended polytopes should be considered as nanotubes.

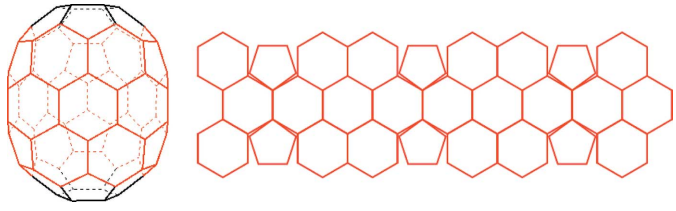

Figure 3
The C_{78}(I) polytope together with its middle belt of the three rows of hexagons and pentagons unwrapped into the plane. Three pairs of vertically aligned pentagons that are linked by a hexagon–hexagon edge single out C_{78}(I).

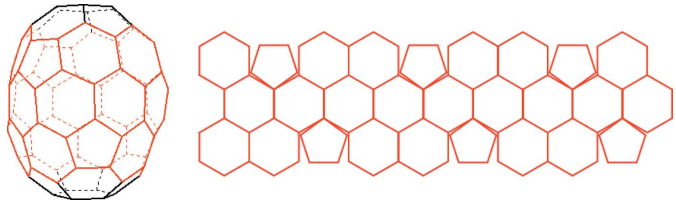

Figure 4
The C_{78}(II) polytope together with its middle belt of the three rows of hexagons and pentagons unwrapped into the plane. Three pairs of pentagons linked by one hexagon single out C_{78}(II).

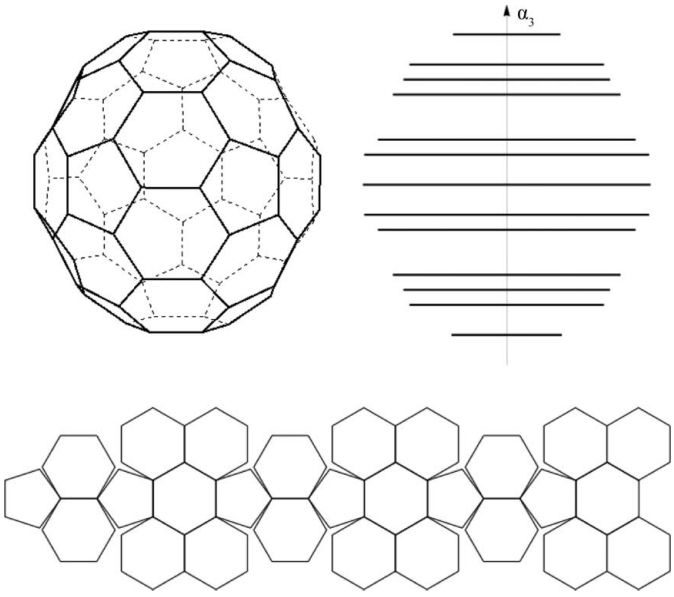

Figure 5
The polytope C_{78}(III) together with its A_2-pancake structure and the middle belt of hexagons and pentagons unwrapped into the plane. Three pairs of horizontally aligned pentagons that are linked by a hexagon–hexagon edge single out C_{78}(III).

When an even number of hexagonal rings is inserted as the middle ring, the lower (or upper) part of the original C_{60} polytope needs to be rotated by the angle $2\pi/18$ in order to match the lower (upper) part of the original polytope.

Polytope C_{78}(II) and its analogs C_{96}, C_{114}, ..., and nanotubes arise in a similar way as in the case of C_{78}(I). Additional rings of nine hexagons can be inserted into the middle of C_{78}(I) and C_{78}(II), see Fig. 7. The greater the number of hexagonal rings inserted, the longer the resulting nanotube that is built.

4.2. Polytope C_{78}(III)

The polytope corresponding to C_{78}(III) shown in Fig. 5 is also a result of symmetry breaking $H_3 \rightarrow A_2$, but is substantially different to C_{78}(I) and C_{78}(II). In those two cases (Figs. 3 and 4) the middle rings of the belts consist of nine hexagons aligned by their faces, while in C_{78}(III) (Fig. 5) the middle ring consists of six pentagons, three hexagons and three edges. In fact C_{78}(III) does not have a ring of nine hexagons oriented in any direction. Therefore it is not amenable to the formation of higher analogs of C_{78} and to nanotubes.

4.3. Polytopes C_{78}(IV) and C_{78}(V)

The polytopes C_{78}(IV) and C_{78}(V) in Fig. 6 can be viewed as combinations of C_{78}(I) and C_{78}(III). Indeed, in their middle belt one finds the formations pentagon–edge–pentagon oriented vertically, as in C_{78}(I), as well as oriented horizontally, as in C_{78}(III). Neither of the two polytopes can be augmented to higher analogs or to nanotubes by the insertion of additional rings of nine hexagons.

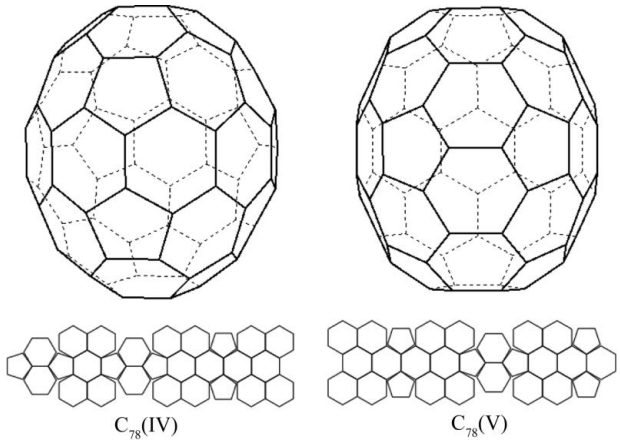

Figure 6
The polytopes C_{78}(IV) and C_{78}(V) and their middle belts of three rows of hexagons and pentagons unwrapped into the plane. Three pairs of pentagons that are linked by a hexagon–hexagon edge single out C_{78}(IV), if two of the pairs are oriented horizontally and one vertically. C_{78}(V) is singled out if two of the pentagon pairs are oriented vertically and the third pair is oriented horizontally.

5. Concluding remarks

The existence of large carbon molecules such as C_{60} led to a search and subsequent discovery of a number of even larger molecules. Considering just the combinatorial possibilities for joining regular pentagons and hexagons on a convex surface, however, leads to a very large number of structures which could be identified (Schwerdtfeger *et al.*, 2013). If in addition, though, certain symmetry properties are required to be respected, the number of possible structures is drastically reduced, producing particular higher carbon molecules in line with those observed in nature.

In the first paper of the series of which this work is a part (Bodner *et al.*, 2013), the mechanisms for production of higher carbon molecular structures utilizing symmetry reduction to a maximal subgroup H_2 of H_3 was studied, namely $H_3 \rightarrow H_2$. In the present paper, we examined a second possibility, which is the symmetry reduction $H_3 \rightarrow A_2$. This reduction to A_2,

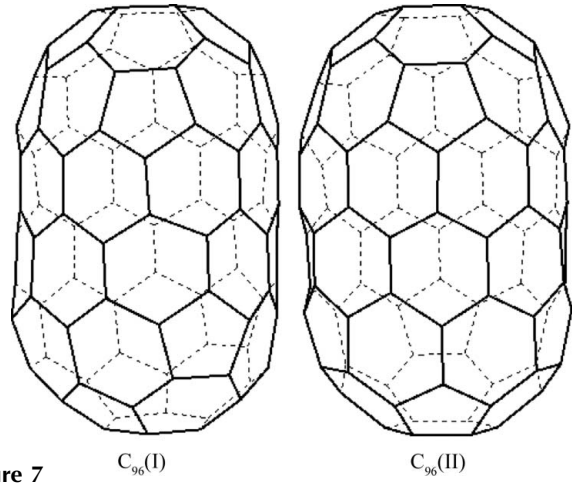

Figure 7
Two carbon structures C_{96} built from C_{78}(I) and C_{78}(II) by adding a ring of nine hexagons into the middle.

however, is not unique as in the reduction to H_2, and there is more than one way to achieve it.

A third possibility for carrying out the symmetry reduction $H_3 \rightarrow A_1 \times A_1$ will be reported elsewhere. This case, like in the case of H_2 symmetry reduction, is unique but is achieved by different means than the insertion of additional belts of hexagons into the middle of the C_{60} surface.

The authors are grateful for the partial support of the work by the Natural Sciences and Engineering Research Council of Canada and by the MIND Research Institute in Irvine, California. MS would like to express her gratitude to the Centre de recherches mathématiques, Université de Montréal, for the hospitality extended to her during her postdoctoral fellowship. She is also grateful to MITACS and OODA Technologies for partial support.

References

Balasubramanian, K. (1991). *Chem. Phys. Lett.* **206**, 210–216.
Bodner, M., Patera, J. & Szajewska, M. (2013). *Acta Cryst.* A**69**, 583–591.
Bodner, M., Patera, J. & Szajewska, M. (2014). *PLoS One*, doi:10.1371/J.pone.0084079.
Cataldo, F., Graovac, A. & Ori, O. (2011). Editors. *The Mathematics and Topology of Fullerenes. (Carbon Materials: Chemistry and Physics)*, Vol. 4. Springer.
Champagne, B., Kjiri, M., Patera, J. & Sharp, R. T. (1995). *Can. J. Phys.* **73**, 566–584.
Dresselhaus, M. S., Dresselhaus, G. & Eklund, P. C. (1996). *Science of Fullerenes and Carbon Nanotubes.* Academic Press.
Fowler, P. W. & Manolopoulos, D. E. (2007). *An Atlas of Fullerenes.* Dover Publications, Inc.
Harris, P. J. F. (1999). *Carbon Nanotubes and Related Structures.* Cambridge University Press.
Lin, Y., Cai, W. & Shao, X. (2006). *J. Mol. Struct. THEOCHEM*, **760**, 153–158.
Lin, Y.-T., Mishra, R. K. & Lee, S.-L. (1999). *Chem. Phys. Lett.* **302**, 108–112.
Ramond, P. (2011). *Group Theory: A Physicist's Survey.* Cambridge University Press.
Schwerdtfeger, P., Wirz, L. & Avery, J. (2013). *J. Comput. Chem.* **34**, 1508–1526.
Szajewska, M. (2014). *Acta Cryst.* A**70**, 358–363.
Wang, D., Shen, H. & Zhai, Y. (2007). *J. Rare Earth.* **25**, 210–214.
Zhang, B. I., Wang, C. Z., Ho, K. M., Xu, C. H. & Chan, C. T. (1993). *J. Chem. Phys.* **98**, 3096–3102.